JOURNAL OF MATERIALS SCIENCE **40** (2005) 5813–5819

Fracture and microstructure of open cell aluminum foam

E. AMSTERDAM, P. R. ONCK, J. TH. M. DE HOSSON*
Department of Applied Physics, Materials Science Center and the Netherlands Institute for Metals Research, University of Groningen, Nijenborgh 4, 9747 AG Groningen, The Netherlands
E-mail: hossonj@phys.rug.nl

SEM and EDS measurements were used to scrutinize the microstructure of Duocel open cell 6101 aluminum foam in relation to its fracture properties. *In-situ* SEM tensile tests on the open cell aluminum foam were performed to investigate the different fracture modes of struts and Aramis/Digital Image Correlation software was used to map the strain in individual struts. Observations during tensile tests showed that the microstructure of the struts has a great influence on the fracture behaviour of the foam. In particular AlFeSi-precipitates, which are due to the casting of the 6101 aluminum alloy, and the morphology of the foam alters the fracture mode of the struts in the foam from transgranular to intergranular. Less energy is needed for intergranular fracture of struts and the strain to failure of the foam is decreased due to weak individual struts.

1. Introduction

This paper concentrates on the relationship between the microstructure and failure behavior of open cell 6101 aluminum foam. When macroscopic forces act on metal foam both compressive and tensile stresses are operating in local areas. Under macroscopic compression metal foams usually exhibit ductile behavior. However, under macroscopic tension the reported strains reached at peak stress are a few percent for open- and closed-cell metal foam [1–9], e.g. an elongation to failure of 5% for a pure aluminum open cell foam and 1–2% for an Al-12Si open cell foam have been reported [1]. The difference in strain at failure e_f is due to the difference in microstructure. In fact, the brittle second phase of Si fractures during deformation in Al-12Si foam, resulting in a much higher damage accumulation rate than in pure aluminum foam [1]. Strains at failure of 1.2% parallel and 2.4% perpendicular to the long axis of the cells have been reported for ERG Duocel open cell aluminum foam [4]. Because detailed information of the effect of the microstructure on the fracture behavior of Duocel open aluminum foam is only scantly available [10] the objective of this paper is to describe the microstructure and the tensile behavior so as to gain insight into the relationship between the tensile behavior and the microstructure for ERG Duocel open cell 6101 aluminum foam.

The paper is organized as follows. In the following section the material is described and the experimental procedures are explained. In the subsequent section the experimental observations are reported followed by a discussion and recommendations.

2. Material and experimental procedures

In this study, ERG Duocel open cell aluminum foam, with 20 pores per inch (PPI), has been examined. Duocel is fabricated from 6101 aluminum alloy using the so-called investment casting technique [11, 12]. A polymer foam is employed as a template, which is filled with a ceramic casting slurry. After baking to burn out the polymer foam template, a ceramic mould is created. Subsequently, the ceramic mould is infiltrated with a liquid aluminum alloy and after resolidification the ceramic is removed and an open cell aluminum alloy foam remains. A consequence of this methodology is that the chemical composition of the 6101 aluminum foam differs from that of bulk 6101 aluminum [10], see Table I. The chemical compositions of both the metal foam and the bulk were reported in [10] using an inductively coupled plasma-atomic emission technique. Although the presence of the elements Pb, Ni and Cr were not reported these elements have been listed in Table I because EDS measurements showed their presence. Also the microstructure of the foam is different from the microstructure of the bulk. In particular the grain size and the size of the secondary phases are both larger in the aluminum foam than in bulk aluminum, which is probably caused by the slow cooling rate of

*Author to whom all correspondence should be addressed.
0022-2461
DOI: 10.1007/s10853-005-4995-8

TABLE I Chemical composition (wt%) of the aluminum alloy before casting (bulk alloy) and after casting of the open cell foam (PPI 20) [10]

Samples	Cu	Mg	Mn	Si	Fe	Zn	B	Pb, Ni, Cr	Al
Bulk alloy	0.04	0.47	0.02	0.29	0.18	0.01	0.04	0.10 max	Balance
PPI 20	0.03	0.29	0.01	0.25	0.14	0.01	0.03	0.10 max	Balance

the foam due to the low thermal conductivity of the ceramic casting slurry.

To investigate *in-situ* the deformation behavior of struts in a scanning electron microscope the aluminum foam samples were cut to the correct size with electro discharging so as to avoid mechanical deformation and the generation of surface defects. *Ex-situ* tensile tests were performed with a tensile machine under displacement control at a rate of 0.5 mm/min. In both cases the foam samples were glued on both sides to aluminum blocks with an epoxy-glue (Araldite 2011) made by Vantico. The aluminum blocks with the foam glued in between could easily be clamped inside the tensile stages without deforming the foam prior to the tensile test. A tensile stage made by Kamrath&Weiss was used for *in-situ* scanning electron microscope (SEM) tensile tests. The displacement rate for *in-situ* tensile tests was 300 μm/min and the maximum dimensions of the foam test samples are 4 $\times$ 10 $\times$ 15 mm (excluding clamping blocks). Foam test samples with these dimensions were used for *in-situ* as well as *ex-situ* tensile tests and all samples were tested with the long axis of the cells parallel to the loading direction. With these dimensions of the test samples and the cell size of 20 PPI it is not possible to have more then 7 cells in height and width of the samples. As a consequence size effects become important because it is only possible to interpret foam specimen as a continuum if the specimen size is more then 7 times the cell size [13, 14].

A Philips/FEI XL30-FEG environmental scanning electron microscope (ESEM) was used for the *in-situ* tensile tests and a Philips/FEI SEM XL30S-FEG was used for further characterization of the microstructure of the aluminum foam. Both SEMs are equipped with detectors to carry out energy-dispersive X-ray spectroscopy (EDS). To investigate grain orientations (Orientation Imaging Microscopy, EBSD/OIM) an electron backscatter detector is attached to the XL30s FEG-SEM. The secondary electron (SE) images and backscatter electron (BSE) images of single struts taken with the SEM during the *in-situ* tensile tests are fed into Aramis/Digital Image Correlation software for strain mapping. The images were taken at certain strain intervals and the tensile stage was stopped to insure a good quality of the image. The applied load was not decreased when the tensile stage was halted.

For optical microscopy examinations the foam samples were embedded in Epo-thin, made by Buehler. This embedding material has the advantage that it is transparent and does not exert internal stress on the open cell foam. The embedded foam samples were polished and etched with Keller's reagent to reveal the grain boundaries. The Keller's reagent also etched away precipitates, which are located at the grain boundary, leaving holes behind. To polish aluminum foam without an embedding material, samples of open cell aluminum foam were electro-chemically polished (ECP). The electrolyte used for ECP of the aluminum foam is A2, made by Struers. The ECP did not remove the precipitates from the grain boundary. In order to examine grain boundaries and the grain size of the aluminum alloy struts, OIM measurements were executed. After electro-chemical polishing the surface became very smooth and suitable for OIM. During ECP material was first removed at the corners of the triangular cross section of the struts and at the grain boundary. At low voltages (<7 V) the foam was etched and at high voltages (>9 V) the ECP was too fast and pitting of the surface was observed.

To examine the effect of precipitates on the fracture mode also artificial struts were manufactured by electro discharging a strut of bulk 6061 aluminum alloy. The shape of the artificial strut was approximately the same as the struts in Duocel open cell foam, i.e. triangular and thicker near the ends.

3. Results

3.1. Microstructural characterization

The length of the struts of the 20 PPI open cell foam ranges from 500 μm to 2 mm and the cross sectional shape of the struts is triangular with round edges. The length of the triangular base ranges from 200 μm for long struts to 400 μm for small struts. Almost all struts consist of one grain through the thickness (see Fig. 1) and 1–3 grains along the length, which means that the shape of the grains is elongated along the length of the struts. The observed grain distributions were confirmed with optical microscopy of an embedded and polished foam sample and with orientation imaging microscopy (OIM). A similar grain structure was also detected in [10, 15]. One strut was found to have a polycrystalline structure with an average grain size of 40–50 μm (see Fig. 2a for a small section of the strut), which was also confirmed with OIM.

The grain structure of the artificial strut was found to be polycrystalline with an approximate grain size of 150–200 μm, being 3–4 times the grain size in the Duocel polycrystalline strut. However, due to the larger dimensions of the artificial strut, the two struts consist of an equal number of grains. Figure 1b represents a BSE image of a grain boundary, which shows precipitates on the grain boundary. However, not every grain boundary contains the same amount of precipitates (see Fig. 1a). EDS measurements indicated that the precipitates are Al-Fe-Si precipitates, which are commonly found in aluminum alloy 6xxx series [16–18]. No precipitates were found in the polycrystalline strut, whereas all grain boundaries of the bulk 6061 aluminum alloy were found to be covered with thin β-AlFeSi-precipitates.

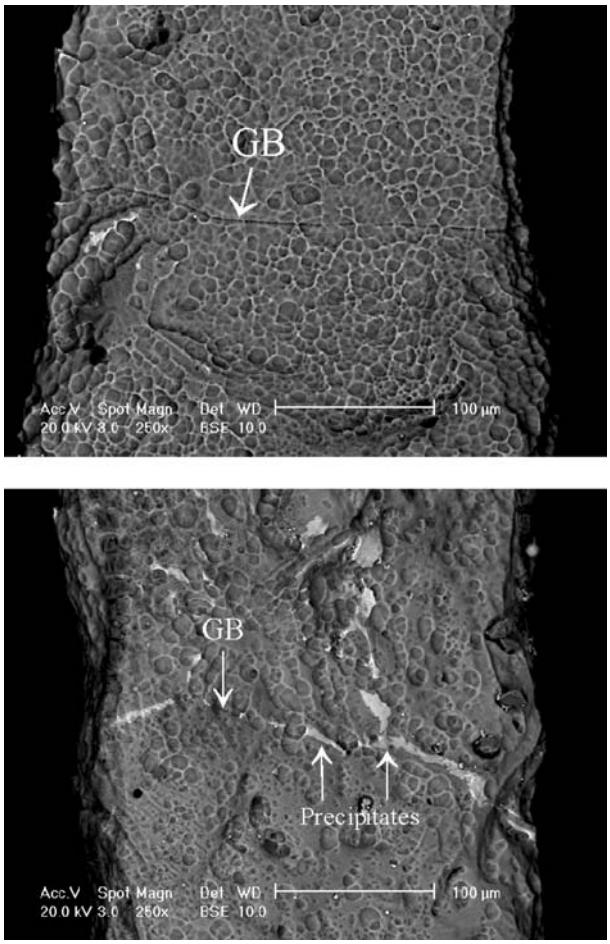

Figure 1 (a) BSE image of a part of a strut with a grain boundary (GB). There are no precipitates on the GB. (b) BSE image of a part of a strut with a grain boundary. The white parts are AlFeSi-precipitates and are located on the GB.

The most common impurity of the alloying additions in the 6xxx series is iron (Fe). Because of the low solid solubility of ∼0.052 wt%, nearly all iron forms second-phase precipitates. The two principal second-phase particles in a silicon-containing alloy are the α-AlFeSi (Al_8Fe_2Si) and the β-AlFeSi (Al_5FeSi) phase. The β-AlFeSi (Al_5FeSi) phase has a monoclinic crystal structure and a plate-like morphology. EDS spectra taken from the β-phase showed a Fe/Si (at.%) ratio of approximately 1 in the chemical composition [16]. The β-AlFeSi has a sharp interface boundary and the highly faceted nature may induce significant stresses in the aluminum matrix acting as a potential site for crack initiation. The α-AlFeSi (Al_8Fe_2Si) has a hexagonal (α_h) or a cubic (α_c) crystal structure and compact Chinese script morphology, with an Fe/Si ratio of about 1.9 [16]. The hexagonal crystal structure forms in alloys with Mn, V or Cr concentrations less than 0.01 wt%, while higher concentrations lead to stabilization of the cubic phase [19, 16]. The α-AlFeSi has a rough or diffuse interface in contact with the aluminum matrix and improves the ductility of the alloy. Which phase (α_h, α_c or β) will form during solidification and the particle size depend on the cooling rate and the exact chemical composition of the aluminum alloy. Besides these two principal phases there are also other stable intermediate phases with stoichiometrical composition $Al_{12-15}Fe_3Si_{1-2}$, reported in [20]. We also observed some of these phases via the Fe:Si ratio obtained with EDS measurements. The formation of the intermetallic phases during equilibrium solidification has been examined in detail and reference is made to [16–19]. The β-phase is dominant at high silicon content and low cooling rates. The size of the AlFeSi-precipitates increases with low cooling rates and scales with the amount of Fe in the aluminum alloy [17, 20–22].

For the Duocel open cell foam the amount of AlFeSi-precipitates clearly differs among various grain boundaries and so does the coverage ratio for the α- and β-phase for the same amount of AlFeSi (see Fig. 1). The fracture toughness of a grain boundary is determined by the coverage ratio, which in turn is determined by the amount of AlFeSi and its phase. Optical microscopy of an embedded and polished foam sample also shows that the total coverage of all grain boundaries in one cross sectional plane is low and non-uniform.

3.2. Fracture behavior

Failure of Duocel open cell foam samples under tensile loading proceeds with the consecutive failure of struts, forming a fracture plane that is more or less perpendicular to the loading direction. Two different failure modes for struts were observed: transgranular and intergranular. The former was found to be more ductile and the latter rather brittle. In the case of transgranular failure the formation of a shear band prior to failure through necking of the strut was detected using DIC (digital image correlation), as can be seen from Fig. 3. The shear band was initiated inside a single grain and the fracture path was transgranular. In contrast, no necking was observed in the case of intergranular failure. Instead, AlFeSi-precipitates were found on both sides of the fracture surfaces suggesting that the crack ran through the AlFeSi-precipitates (see Fig. 2b–d). An internal report, about single strut tensile tests, shows that intergranular fracture of a single strut occurs before the peak stress of the transgranularly fractured strut and therefore less energy is needed for the intergranular fracture of a strut than for transgranular fracture of a similar strut [23].

The Duocel polycrystalline strut without precipitates on the grain boundaries was also deformed *in-situ* to observe failure. During the tensile test the strut fractured transgranularly and substantial necking was observed before failure. Also slip bands were clearly visible. Two polycrystalline artificial struts with grain boundary precipitates were tested under uniaxial tension and both samples fractured without visible plastic deformation. All fracture surfaces were covered with AlFeSi-precipitates, indicating intergranular fracture. From the above it can be concluded that grain boundaries without precipitates are stronger and precipitates contribute to intergranular failure.

The fracture surfaces of struts in the Duocel foam that show intergranular failure are all covered with AlFeSi-precipitates and EDS measurements show that

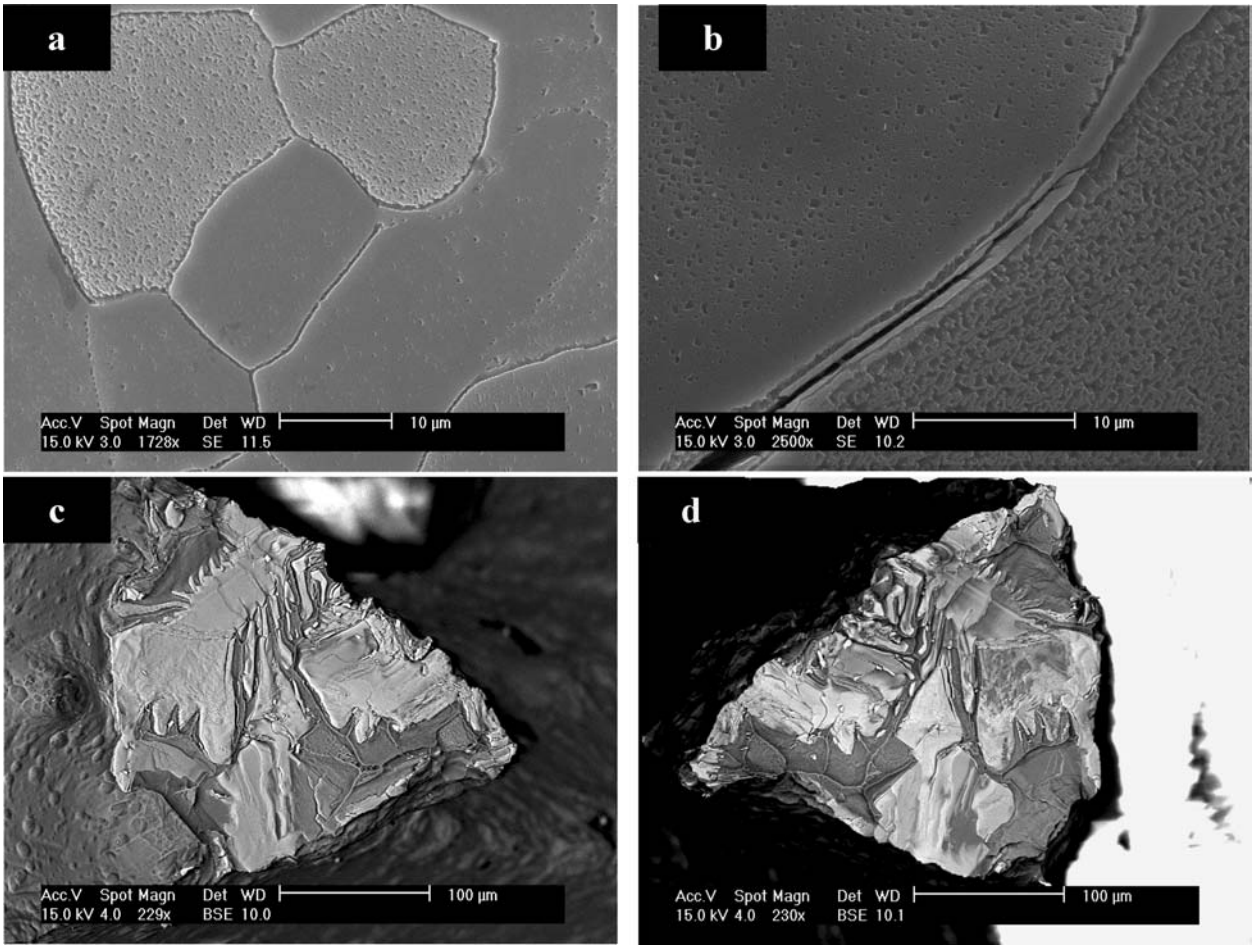

Figure 2 (a) Grain structure of the polycrystalline strut revealed by electro-chemical polishing that caused pitting. The pitting depends on the orientation of the grains and therefore each grain has a different amount of pitting and a different contrast in the SE image. (b) SE image of an electro-chemically polished (ECP) strut. ECP does not remove the AlFeSi-precipitates and the difference in pitting for different grain orientations is clearly visible. The crack associated with intergranular fracture runs through the AlFeSi-precipitates and sometimes over the interface with the aluminum. (c), (d) BSE images of the fracture surface of the upper part (c) and lower part (d) of a fractured strut. The fracture surface is covered with β-AlFeSi and additional Si, indicating that the fracture was intergranular. Most of the surface area has failed by cleavage of the precipitates, while a small portion has failed by debonding along the precipitate-matrix interface.

the Fe:Si ratio of the precipitates lies between 1:1 and 1:2. The phase is likely to be β-AlFeSi with additional Si. Near the edges of the strut also Fe:Si ratios between 2:1 and 3:2 were sometimes measured, indicating that α-AlFeSi is also present at particular sites. From the literature [1] it is known that Si is a very brittle phase, and it will probably decrease the strength of the plate-like β-AlFeSi. The amount of AlFeSi-precipitates clearly differs among various grain boundaries and so does the coverage ratio for the α- and β-phase for the same amount of AlFeSi (see Fig. 1).

Observations during 3 *ex-situ* tensile tests on small open cell foam samples, pointed out that bending is the dominant deformation mechanism as a result of which the struts effectively rotate to become more aligned with the loading direction. Struts that are already aligned in this direction can only stretch and the amount of strain depends on the local topology. If one of these struts contains a weak grain boundary and a highly realigning surrounding, this strut will fracture first. Fig. 4 displays the fracture plane of a small foam sample; the numbers indicate fractured struts and strut number 1 fractured first. In all samples the first strut that fractures fails intergranularly. After fracture of the first strut the applied load is redistributed over the remaining struts and if some of the surrounding struts also contain weak grain boundaries that cannot withstand the applied load, they will fracture as well. Strut #2 fractured transgranularly and strut #3 fractured intergranularly before the peak stress was reached. A notch is being created and the stress on the remaining struts in the fracture plane increases. Stronger struts in the fracture plane also start to fail transgranularly as the applied load increases. After the transgranular fracture of struts 4, 5, 6 and 7 the stress of the foam sample decreases and the realignment of the struts in the rest of the foam stops. The stress is shifted to the remaining struts that hold the two ends of the foam together. These struts fail either transgranularly (#10) or intergranularly (#8, 9, 11). Near the end of the tensile test most strut have failed either in a intergranular or transgranular manner and only one strut holds the two pieces of foam still together. This last strut #12 reorientates itself in the loading direction and it strains until it fails transgranular upon increasing the applied displacement.

In all samples we investigated the first strut fails intergranularly, while the last strut often fails transgranularly. This is in accordance with the long tail of the tensile stress strain curves, often observed for relatively

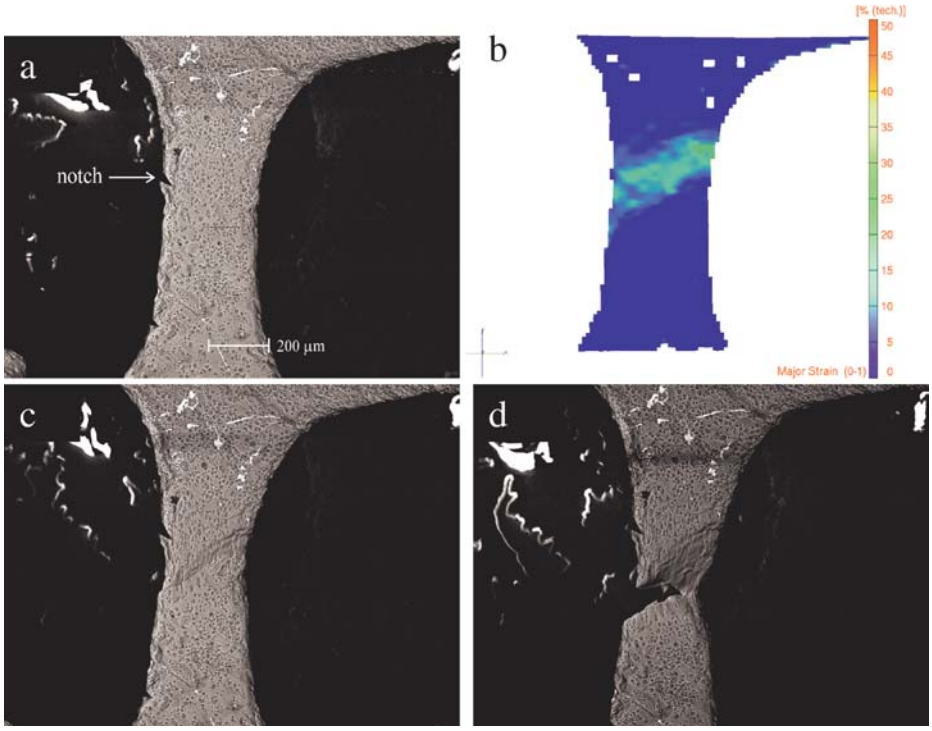

Figure 3 (a) BSE image of a strut during an *in-situ* tensile test with a small amount of deformation, but before plastic localization. (b) Principal strain distribution inside the strut; A shear band is clearly visible. Strain was calculated with Aramis by comparing the image of 3a with an image of the same strut prior to deformation. The white rectangles inside the strut are areas for which Aramis could not give an accurate correlation. (c) Ductile fracture of the strut of figure (a) during the *in-situ* tensile test. The location of the shear band is not influenced by the incision made with a surgical blade. (d) Ultimate transgranular failure.

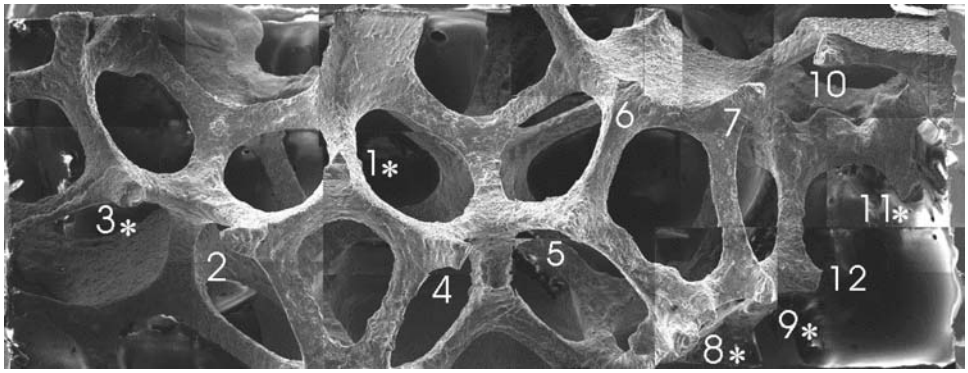

Figure 4 Fracture plane of Duocel open cell foam. The numbers indicate the consecutively failed struts and the stars indicate intergranular fracture.

ductile foams. Fig. 5 shows two histograms plotting the frequency of the occurrence of intergranular and transgranular strut failure as a function of location along the struts and initial orientation for the 3 samples analyzed. In total 37% of all struts fail in an intergranular manner. Despite the limited amount of struts analyzed, two trends can be observed: (i) most struts that have failed in either an intergranular or transgranular manner were initially aligned in the loading direction and (ii) most transgranular struts failed half way the strut axis. The first trend is probably a consequence of the fact that the applied strain is accommodated by bending of struts that are not aligned with the loading direction, while it is accommodated by uniaxial stretching in case of aligned struts. In the latter case a full plastic cross section is attained at a smaller applied strain [24], while stresses are high throughout the entire length of the strut. Due to the uniformly high stresses all possible locations of weak (precipitation-covered) boundaries are probed, ultimately resulting in intergranular failure at a random position along the strut (cf. Fig. 5).

Simulations have shown that stress peaks occur at 20% and 80% of the length of the strut under combined shear/tensile loading and *in-situ* observations indeed indicate plasticity yielding at these places under shear loading [25]. Two polycrystalline artificial struts with precipitates on the grain boundaries fractured intergranularly at 20% or 80% of their length under shear/tensile loading. Therefore a strut inside the foam under shear loading with a weak grain boundary at 20% or 80% of the length of the strut may fracture intergranularly due to the non-uniform stress distribution, while in pure tension the strut would fracture in a ductile manner at the thinnest part of the strut. Clearly, besides the non-uniform chemical composition and cooling rate of the whole foam also the local topology and geometry of the struts have an effect on the failure mode of the metal foam.

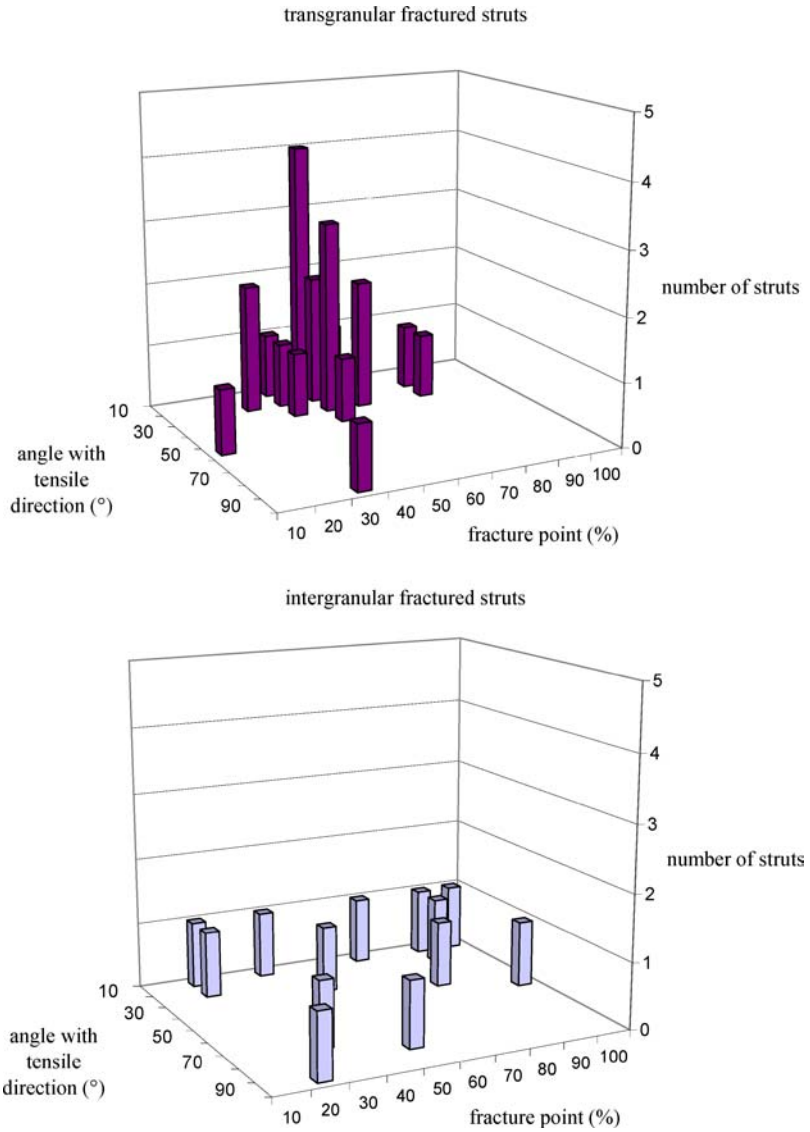

Figure 5 Statistics showing the relation between the location of fracture along the strut and the angle with the tensile direction prior to deformation of transgranular (a) and intergranular (b) fractured struts. A fracture point of 50% means that the strut fractured half way and 0% or 100% means at the vertex.

4. Discussion

In order to enhance the transgranular/intergranular fracture ratio the fracture toughness of the grain boundaries of the intergranularly fractured struts has to be improved. When the grain boundary coverage of AlFeSi-precipitates decreases, this ratio is bound to increase. The coverage can be altered in two different ways: by influencing the volume fraction of precipitates and by influencing the phase of the AlFeSi-precipitates.

Decreasing the concentration of Fe in the alloy will decrease the concentration of AlFeSi-precipitates, since this concentration scales with the amount of Fe and not of Si. Fe is an unwanted alloying impurity but its presence is hard to avoid. The amount of Fe can only be decreased by using rather pure starting materials (leading to an increase of the costs). The concentration of AlFeSi-precipitates also scales with the cooling rate. The concentration of AlFeSi-precipitates decreases with increasing cooling rates [21, 22].

When the phase of the precipitates changes from β-AlFeSi to α-AlFeSi, the coverage decreases due to the morphology of the α-phase. The formation of the α-phase can be promoted by heat treatment of the foam or by adding certain transition elements to the alloy prior to the solidification. Heat treatment using an extended homogenization procedure changes most of the β-phase into the α-phase [17]. However, also the aluminum matrix changes due to heat treatments, so that the overall effect on the ductility is to be awaited. Heat-treated samples of Duocel open cell foam, for instance, were more brittle during compression tests than untreated samples [10]. Addition of transition elements such as Mn, Cr, Co and Sr promote the formation of the α-phase during solidification of the aluminum alloy [16]. It is thought that Sr is adsorbed at the α-AlFeSi/aluminum interface, thus preventing the diffusion of Si into the α-AlFeSi as the temperature decreases during solidification.

In Duocel foam the transgranular failure of struts is initiated by plastic localization, such as shear band formation and necking. Since plastic localization is postponed when strain hardening is more pronounced, it is expected that the ductility of transgranularly failing foam is enhanced when struts are polycrystalline

instead of single crystalline (in thickness) [26]. Indeed, some parts in the Duocel foam were found to be polycrystalline, without grain boundary particles. Since the grain size and the size of the secondary phases are inversely proportional to the cooling rate, a locally enhanced cooling rate could have caused this. Another possibility is that the cooling rate was the same as in the rest of the foam, but the chemical composition differs so that precipitates could not be formed.

5. Conclusion

Casting of 6101 aluminum open cell foam introduces intermetallic phases into the microstructure. The intermetallic phases, which are primarily α- and β-AlFeSi-precipitates, are located at the grain boundary and alter the fracture mode of struts from transgranular to intergranular. The fracture surfaces of the brittle fractured struts were covered with β-AlFeSi-precipitates to a large extent. Due to the plate-like shape and the low fracture toughness of the β-AlFeSi-precipitates, the toughness of grain boundaries is decreased which leads to intergranular fracture of struts. As a result of the non-uniform distribution of the precipitates a portion of the struts in the fracture plane of the foam fails intergranularly and the energy required for intergranular fracture of a strut is less than for transgranular fracture. The non-uniform stress distribution inside a strut under shear loading, in combination with the precipitation on the grain boundary, can also cause struts to fail intergranularly. In total 37% of the struts in a fracture plane fail intergranularly. The intergranular fracture of the struts due to the β-AlFeSi-precipitates decreases the strain to failure of the entire aluminum foam. According to literature the grain boundary coverage of AlFeSi-precipitates can be reduced by heat-treatment, reduction of Fe concentration and addition of transition elements.

Acknowledgements

Financial support from the Foundation for Fundamental Research on Matter (FOM-Utrecht) and the Netherlands Institute for Metals Research is gratefully acknowledged.

References

1. C., San Marchi, J.-F. Despois Mortensen *A. Acta Mater.* **52** (2004) 2895.
2. A.-M., Harte N. A., Fleck and M. F. Ashby *Acta Mater.* **47** (1999) 2511.
3. Y., Sugimura J., Meyer M. Y., He ., Bart-Smith J.,HGrenestedt Evans A.G. *Acta Mater.* **45** (1997) 5245.
4. E., Andrews W., Sanders L. J. Gibson *Mater. Sci. Eng.* **A270** (1999) 113.
5. A. E., Markaki T. W. Clyne *Acta Mater.* **49** (2001) 1677.
6. O. B., Olurin N. A., Fleck M. F. Ashby *Mater. Sci. Eng.* **A291** (2000) 136.
7. C., Motz R. Pippan *Acta Mater.* **50** (2002) 2013.
8. C., Motz R. Pippan *Acta Mater.* **49** (2001) 2463.
9. K. Y. G., McCullough N. A., Fleck M. F. Ashby *Acta Mater.* **47** (1999) 2323.
10. J., Zhou C., Mercer W. O. Soboyejo *Met. Trans.* **33A** (2002) 1413.
11. J. Banhart *Prog. Mater. Sci.* **46** (2001) 559.
12. M. F., Ashby A. G., Evans N. A., Fleck L. J., Gibson J. W., Hutchinson H. N. G. Wadley Metal Foams: A Design Guide. Butterworths, Londen, 2000.
13. P. R., Onck E. W., Andrews L. J. Gibson *Int J Mech. Sci* **43** (2001) 681.
14. E. W., Andrews, g., Gioux, P. R., Onck, L. J. Gibson, *Int. J. Mech. Sci.* **43** (2001) 701–713.
15. T. G., Nieh K., Higashi J. Wadsworth *Mater. Sci. Eng.* **A283** (2000) 105.
16. M. H., Mulazimoglu A., Zaluska J.E., Grusleski F. Paray *Met. Trans.* **27A** (1996) 929.
17. F. H., Samuel A. M., Samuel H. W., Doty S. Valtierra *Met. Trans.* **32A** (2001) 2061.
18. G., Sha O'K. A. Q., Reilly B., Cantor J. M.,Titchmarsh R. G. Hamerton *Acta Mater.* **51** (2003) 1883.
19. Kuijpers N. C. W. Kinetics of the β-AlFeSi to α-Al(FeMn)Si transformation in Al-Mg-Si alloys. PhD thesis, Technical University Delft, Delft, 2004.
20. W., Khalifa F. H., Samuel J. E. Gruzleski *Met. Trans* **34A** (2003) 807.
21. B., Dutta M. Rettenmayr *Mater. Sci. Eng.* **A283** (2000) 218.
22. B., Dutta M. Rettenmayr *Mater. Sci. Technol.* **18** (2002) 1428.
23. A. Raaijmakers Fracture behaviour of open cell foams. Master Thesis, University of Groningen, Groningen, 2003.
24. L. J., Gibson M. F. Ashby Cellular Solids: Structure and Properties. Pergamon Press, Oxford, 1988.
25. P. R., Onck, R., van Merkerk J. T. M. De Hosson & Schmidt I. *Adv. Eng. Mater.* **6** (2004); 429.
26. V., Goussery Y., Bienvenu S., Forest A.-F., Gourgues C.,Colin J.-D. Bartout *Adv. Eng. Mater.* **6** (2004) 432.

Received December 2004
and accepted April 2005